Spray Processable Hybrid 3,4-Propylenedioxythiophene: Phenylene Electrochromic Polymers

Emilie M. Galand,† Jeremiah K. Mwaura,† Avni A. Argun,† Khalil A. Abboud,† Tracy D. McCarley,‡ and John R. Reynolds*,†

The George and Josephine Butler Polymer Research Laboratory, Department of Chemistry, Center for Macromolecular Science and Engineering, University of Florida, Gainesville, Florida 32611, and Department of Chemistry, Louisiana State University, Baton Rouge, Louisiana 70803

Received March 2, 2006; Revised Manuscript Received June 22, 2006

ABSTRACT: The optical and redox properties of a new family of thiophene−phenylene-based molecules are reported. The monomers 1,4-bis[2-(3,3-dimethyl-(3,4-propylenedioxy)thienyl]-2,5-didodecyloxybenzene (BProDOT-Me_2-$B(OC_{12}H_{25})_2$) and 1,4-bis[2-(3,3-dihexyl-(3,4-propylenedioxy)thienyl]-2,5-didodecyloxybenzene (BProDOT-Hex_2-$B(OC_{12}H_{25})_2$) have been synthesized via Negishi coupling of the alkyl-substituted ProDOT and didodecyloxyphenylene units in ca. 40% yields. They were efficiently electropolymerized to form electroactive films which exhibit redox switching at fairly low potentials (∼+0.1 V vs Fc/Fc^+). BProDOT-Hex_2-$B(OC_{12}H_{25})_2$) was polymerized via ferric chloride-mediated chemical oxidation and the polymer isolated after dedoping with hydrazine. A number-average molecular weight of 14 600 g/mol was estimated using size exclusion chromatography, and the polymer structure was confirmed by MALDI mass spectrometry. The polymer is highly soluble in chloroform, THF, and toluene, and homogeneous films were prepared by spin-coating or spray-casting from a chloroform solution. Electronic band gaps of 2.1 eV have been characterized spectroelectrochemically for both the methyl- and hexyl-substituted polymers from the onset of the π to π^* transition. PBProDOT-Hex_2-$B(OC_{12}H_{25})_2$ electrochemically switches between orange, blue, and highly transmissive-gray colors, making it potentially useful in large area electrochromic displays. It also exhibits solvatochromic properties, being yellow in good solvents and red in poorly solvating solvents. Polymer light-emitting diodes have been prepared with PBProDOT-Hex_2-$B(OC_{12}H_{25})_2$ and have shown a strong yellow emission with $\lambda_{max} = 570$ nm. The current−voltage characteristics of PBProDOT-Hex_2-$B(OC_{12}H_{25})_2$-based hole-only devices have also been measured and fitted to the space charge limited current model, allowing a direct measurement of the hole mobility which has been determined to be ca. $10^{-7}-10^{-6}$ cm^2 V^{-1} s^{-1}.

Introduction

Thiophene−phenylene-based copolymers have been extensively studied for their interesting electrical and optical properties such as redox electroactivity and electrochromism, reactivity to chemical sensing, charge transport, and light emission.[1−13] In addition, the various coupling reactions available for heterocycles and the variety of methods for the polymerization of thiophene-based monomers render them fairly easy to synthesize. Phenylene rings are particularly convenient to derivatize with variable substituents, and their subsequent polymerization yields materials with controllable band gaps and solubilities.[4−6] Narrowing of the band gaps in hybrid thienylene−phenylene polymers has been observed by replacing alkyl groups with alkoxy groups due to an increased electron density and reduced steric effect brought by the electron-donating oxygen atoms. For instance, a band gap of 3 eV for poly(2,5-dihexyl-1,4-bis-(2-thienyl)phenylene) is reduced to 2.4 eV for the analogous alkoxy-derivatized polymer.[5]

The attachment of an ethylenedioxy bridge between the 3- and 4-positions of the thiophene broadens the range of band gaps available for the thienylene−phenylene-based polymer family. These materials are highly electron rich with very low oxidation potentials which allows milder oxidative polymerization conditions and the formation of more stable polymers.[4,7] As an example, a series of poly[1,4-bis[2-(3,4-ethylenedioxythienyl)]-2,5-dialkoxybenzenes] (PBEDOT-$B(OR)_2$) with band-gap values between 1.75 and 2.0 eV and polymer half-wave potentials as low as −0.4 V vs ferrocene (Fc/Fc^+) have been reported[4,8] (assuming that the half-wave potential ($E_{1/2}$) of $Fc/Fc^+ = 0.38$ V vs the saturated calomel electrode (SCE) and $E_{1/2}$ of $Ag/Ag^+ = 0.26$ V vs SCE).[14] However, these polymers have been only synthesized by electrochemical methods, and the attempted ferric chloride-mediated chemical polymerizations have led to poorly soluble materials difficult to characterize and to process.[4] With the emergence of soft and flexible plastic devices for use in solar cells, electrochromic devices, or light-emitting diodes (LEDs), it is of great interest to synthesize neutral soluble conjugated polymers which can be processed directly from a solution into thin films for instance by spray-casting or spin-coating. Our group made a recent impact in this field with the development of spray-coatable electrochromic 3,4-propylenedioxythiophene (ProDOT) polymers.[15] Similar to ethylenedioxythiophene (EDOT)-based monomers, the oxygen atoms of the propylenedioxy bridge increase the electron density of the thiophene ring and lower its oxidation potential. Indeed, the ProDOT oxidation peak was reported[16] around +0.98 V vs Fc/Fc^+ while thiophene oxidation was reported[17] around +1.22 V vs Fc/Fc^+ and the EDOT oxidation peak is found[18] at +0.88 V vs Fc/Fc^+ for comparison. The effect of the electron-donating oxygens on the oxidation potential is a bit less for ProDOT than for EDOT due to its twisting conformation, which diminishes the overlap between the oxygen lone pairs and the aromatic thiophene ring. In continuation of our work on electrochromic isoregic poly[1,4-bis(2-thienyl)dialkoxyphen-

† University of Florida.
‡ Louisiana State University.
* Corresponding author: E-mail: reynolds@chem.ufl.edu.

10.1021/ma060466n CCC: $33.50
Published on Web 09/19/2006

Scheme 1

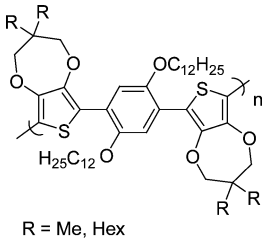

ylenes],[5,6] we decided to take advantage of the ProDOT properties by using it as the polymerizable moiety.

We report here the synthesis of methyl-substituted (R = Me) and hexyl-substituted (R = Hex) poly[1,4-bis[2-(3,4-propylenedioxythienyl)]-2,5-didodecyloxybenzene] [PBProDOT-R_2-B($OC_{12}H_{25}$)$_2$] shown in Scheme 1, with the methyl-substituted molecule studied for comparison with the more soluble hexyl-derivatized molecule. Both polymers were prepared by electropolymerization while the BProDOT-Hex_2-B($OC_{12}H_{25}$)$_2$ monomer was also polymerized by chemical oxidation using ferric chloride to yield a polymer highly soluble in organic solvents. ^{1}H NMR spectroscopy confirmed the polymerization with the disappearance of end-group peaks, and MALDI mass spectrometry confirmed the polymer structure with a spacing between the peaks corresponding to the repeat unit of the polymer. A number-average molecular weight of near 15 000 g mol^{-1} has been determined by GPC. Thin films were deposited via spray-casting the polymeric solution onto working electrodes, and the optoelectronic properties and electrochemical properties were studied. The polymer exhibits electrochromic and solvatochromic properties, which were studied in this report. A preliminary investigation utilizing this polymer as an emitter in light-emitting diodes (LEDs) is also included. Finally, the hole transport properties of PBProDOT-Hex_2-B($OC_{12}H_{25}$)$_2$ were investigated using the space charge limited current (SCLC) model.

Results and Discussion

Monomer Synthesis. Monomers BProDOT-Me_2-B($OC_{12}H_{25}$)$_2$ and BProDOT-Hex_2-B($OC_{12}H_{25}$)$_2$ were synthesized from 1,4-dibromo-2,5-didodecyloxybenzene and the corresponding substituted ProDOT unit by Negishi coupling. Williamson etherification was used to prepare 1,4-dibromo-2,5-didodecyloxybenzene from 1,4-dibromo-2,5-dihydroxybenzene and 1-bromododecane.[4] The substituted 3,4-propylenedioxythiophene (ProDOT) derivatives were synthesized by transetherification of 3,4-dimethoxythiophene and the dialkyl-substituted propane-1,3-diols as previously reported.[15] The ProDOT derivatives were lithiated with 1 equiv of *n*-butyllithium and reacted with $ZnCl_2$. Coupling with 1,4-dibromo-2,5-didodecyloxybenzene was first attempted using tetrakis(triphenylphosphine)palladium(0) [Pd(PPh_3)$_4$] as the catalyst as previously reported for EDOT and thiophene derivatives[4,5] but was limited possibly by unfavorable steric interactions between the heterocycles. However, the Negishi coupling was more successful using a different catalyst system made of commercially available $Pd(0)_2(dba)_3$ and tri-*tert*-butylphosphine ligands [P(*t*-Bu)$_3$] which has been proven very efficient for coupling sterically demanding molecules.[19] Both monomers were obtained in decent yields (ca. 40%) after purification by column chromatography and were characterized by UV−vis, ^{1}H NMR, ^{13}C NMR, melting point determination, elemental analysis, and HRMS. As expected, the monomer containing long and flexible hexyl chains melts at a lower temperature (45−46 °C) than the methyl-substituted monomer (80−82 °C). BProDOT-Me_2-B($OC_{12}H_{25}$)$_2$ and BProDOT-Hex_2-B($OC_{12}H_{25}$)$_2$ exhibit similar absorption maxima in toluene at 354 and 356 nm, respectively, with extinction coefficients of 16 430 M^{-1} cm^{-1} for the former and of 15 640 M^{-1} cm^{-1} for the latter. Replacement of the methyl groups by the longer hexyl chains does not lead to any observable change in the monomer's optical properties.

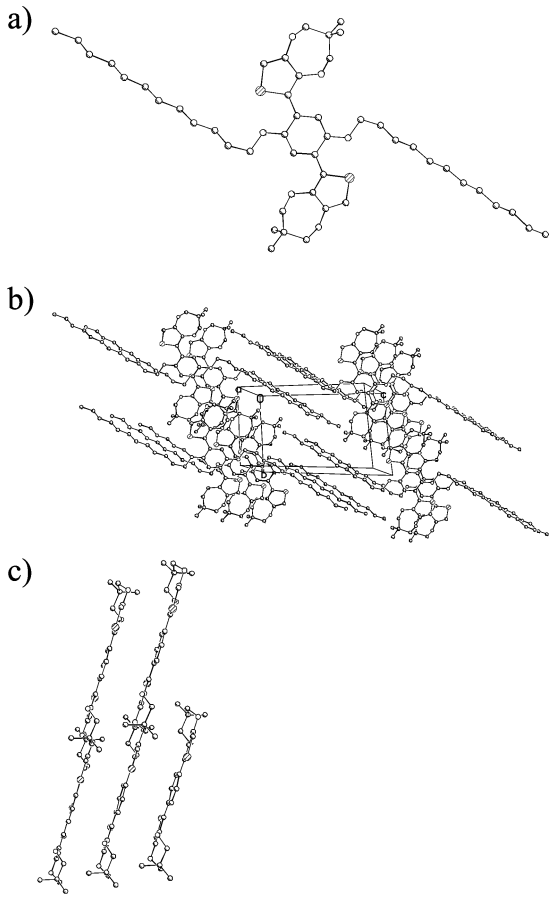

Figure 1. (a) Molecular structure, (b) packing mode of BProDOT-Me_2-B($OC_{12}H_{25}$)$_2$ single crystals, and (c) π-stacking of BProDOT-Me_2-B($OC_{12}H_{25}$)$_2$ illustrated without the phenylene side chains ($OC_{12}H_{25}$).

Structural Analysis. Suitable crystals for an X-ray diffraction study to determine the crystal structure of BProDOT-Me_2-B($OC_{12}H_{25}$)$_2$ were obtained from a hexanes/ethyl acetate mixture (3/1 ratio). BProDOT-Me_2-B($OC_{12}H_{25}$)$_2$ crystallizes in the triclinic *P*-1 space group. The molecular structure is shown in Figure 1a and the packing mode in Figure 1b,c. The molecules, which are located on inversion centers, are nearly planar with a dihedral angle of 6.6° between the central phenyl and thiophene rings. Molecular planarity is a desirable feature since less energy is required to stabilize the bipolaron state upon polymer oxidation. The molecules stack with a small perpendicular distance of 3.679 Å between the central phenyl rings of adjacent molecules, as evident in Figure 1c. If this extended to the polymers, such a small intermolecular distance would favor interchain transport and these materials might represent good candidates for devices requiring high charge mobility such as field effect transistors. While X-ray results are not available at this time, we are developing oligomers as models of these polymers, and future work is directed to comparing the structures of the monomers, oligomers, and polymers to see whether they exhibit similar packing. BProDOT-Hex_2-B($OC_{12}H_{25}$)$_2$ crystals were not of sufficient size for single-crystal structure analysis.

Electropolymerization. The two monomers were electrochemically polymerized on a platinum (Pt) button electrode

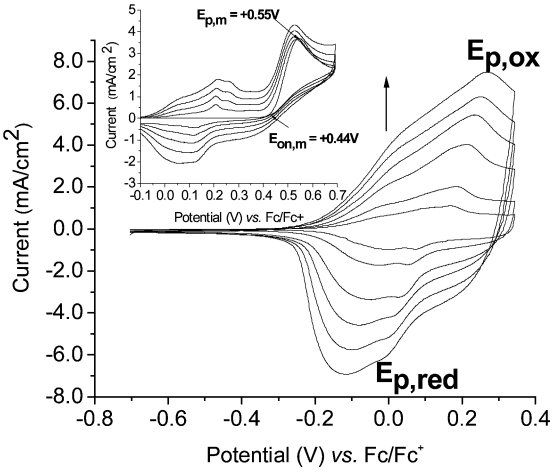

Figure 2. Cyclic voltammograms of PBProDOT-Me_2-$B(OC_{12}H_{25})_2$ (in 0.1 M TBAP in CH_3CN/CH_2Cl_2 (5/3)) at scan rates of 25, 50, 100, 150, 200, and 250 mV s^{-1}; the left top inset shows the repeated potential scanning electropolymerization of BProDOT-Me_2-$B(OC_{12}H_{25})_2$ (0.01 M, saturated solution in 0.1 M TBAP in CH_3CN/CH_2Cl_2 (5/3)) at a scan rate of 50 mV s^{-1}.

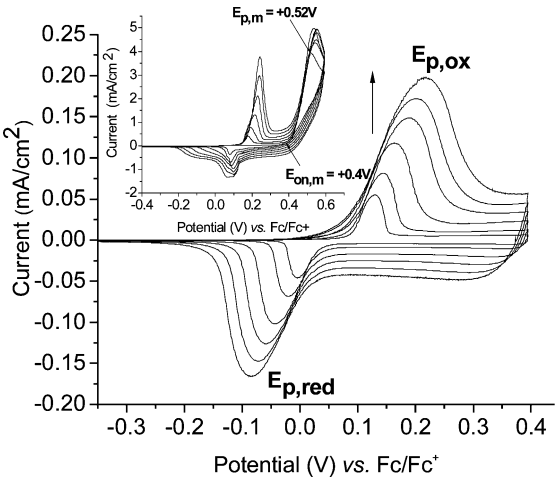

Figure 3. Cyclic voltammograms of PBProDOT-Hex_2-$B(OC_{12}H_{25})_2$ (in 0.1 M TBAP in CH_3CN/CH_2Cl_2 (5/3)) at scan rates of 25, 50, 100, 150, 200, and 250 mV s^{-1}; the left top inset shows the repeated potential scanning electropolymerization of BProDOT-Hex_2-$B(OC_{12}H_{25})_2$ (0.01 M, saturated solution in 0.1 M TBAP in CH_3CN/CH_2Cl_2 (5/3)) at a scan rate of 50 mV s^{-1}.

using an acetonitrile (CH_3CN)/dichloromethane (CH_2Cl_2) (5/3) solution with 0.1 M tetrabutylammonium perchlorate (TBAP) and saturated in monomer (0.01 M). Dichloromethane was required due to the poor solubility of the monomers in CH_3CN. However, too much CH_2Cl_2 hindered polymer formation, and deposition on the electrode and only the use of monomer saturated solution helped to circumvent that problem. The repeated scanning electropolymerizations of BProDOT-Me_2-$B(OC_{12}H_{25})_2$ and of BProDOT-Hex_2-$B(OC_{12}H_{25})_2$ are shown in Figures 2 and 3, respectively. During the first anodic scan, a single peak is observed which corresponds to irreversible monomer oxidation and formation of cation radicals. The peaks of monomer oxidation ($E_{p,m}$) are observed at +0.55 V for BProDOT-Me_2-$B(OC_{12}H_{25})_2$ and at +0.52 V for BProDOT-Hex_2-$B(OC_{12}H_{25})_2$ vs Fc/Fc^+. (All further potentials will be reported versus this reference electrode.) With repeated potential scanning, a polymer film grows onto the electrode surface in both cases. Cathodic and anodic redox processes are observed during polymer reduction and oxidation, and both increase in intensity with repeated scanning indicative of a successful effective electroactive polymer film deposition. The oxidation potential of the polymer also increases with film thickness due to the increase in polymer resistance.

The polymer films formed on the electrode were rinsed with a monomer-free solution of CH_3CN/CH_2Cl_2 (5/3) in which films are not soluble, and cyclic voltammograms were further recorded with scan rate values ranging from 25 to 250 mV s^{-1} (Figures 2 and 3). A linear relationship is observed between the current and the scan rate, indicating that the film is electrode supported and electroactive. The redox processes for the BProDOT-Me_2-$B(OC_{12}H_{25})_2$ system are broad and overlap well as expected for a nicely electroactive polymer, with the peak oxidation ($E_{p,ox}$) and reduction ($E_{p,red}$) potentials around +0.25 and −0.01 V, respectively, at 100 mV s^{-1}. However, $E_{p,ox}$ and $E_{p,red}$ for PBProDOT-Hex_2-$B(OC_{12}H_{25})_2$ (+0.16 and −0.04 V, respectively, at 100 mV s^{-1}) are highly separated as the longer and bulkier chains on the hexyl-substituted ProDOT inhibit the fast movement of counterions. The electrochemical results are summarized in Table 1. Both molecules have similar electrochemical values, with half-wave potentials around +0.05−0.1 V, which shows that functionalizing the ProDOT unit with long solubilizing hexyl chains has little influence on the electronic properties. These potentials are lower than the values measured for the analogous 1,4-bis(2-thienyl)-2,5-diheptoxybenzene polymer, which exhibits[6] an $E_{1/2}$ value of +0.36 V vs Fc/Fc^+, showing the effect of the electron donating oxygens of the ProDOT unit on the polymer oxidation potential. A lower $E_{1/2}$ of −0.40 V vs Fc/Fc^+ has been reported for the analogous 1,4-bis(3,4-ethylenedioxythienyl)-2,5-didodecyloxybenzene polymer due to the stronger electron-donating effect of EDOT.[4]

Oxidative Solution Polymerization. The chemical polymerization of BProDOT-Hex_2-$B(OC_{12}H_{25})_2$ was carried out by addition of a ferric chloride slurry ($FeCl_3$, 3 equiv) in chloroform to a chloroform solution of the monomer over a 2 h period. The polymerization was carried out overnight at room temperature, and the oxidized polymer was then precipitated in cold methanol, collected, and dissolved in chloroform and stirred for 6 h with about 10 mL of hydrazine monohydrate to reduce the polymer into its neutral form. The neutral polymer was precipitated one more time in cold methanol, filtered through a cellulose thimble, and purified by Soxhlet extraction with methanol as the refluxing solvent to remove unreacted monomer and inorganic impurities. Final extraction with chloroform afforded a red solid in 92% yield after solvent evaporation. The polymer is soluble in common organic solvents such as THF, dichloromethane, chloroform, and toluene. ^1H NMR shows broad signals, and the signals of the ProDOT proton end groups essentially disappear as expected for polymerization to a substantial degree (compare ^1H NMR spectra of monomer and polymer in the Supporting Information). As structure proof, the polymer was characterized by MALDI mass spectrometry using a terthiophene matrix. Hydrogen end groups were observed, and the spacing between the peaks corresponds to ∼1090 amu, which corresponds to the calculated molecular weight of the repeat unit of the polymer. Iron and chlorine were efficiently removed as demonstrated by elemental analysis, which shows the presence of only 1 iron per 50 sulfurs and of 1 chlorine per 42 sulfurs. Molecular weight (MW) analysis performed by GPC (polystyrene standards, THF as mobile phase) gave a number-average molecular weight of 14 600 g mol^{-1} and a weight-average molecular weight of 23 000 g mol^{-1} with a polydispersity index of 1.6. As illustrated in Figure 4, polymer elution was monitored with an in-line photodiode array detector to record the UV−vis absorption of selected fractions of the polymer. Spectra were recorded at various times which allowed

Table 1. Electrochemical Results for BProDOT-R_2-$B(OC_{12}H_{25})_2$ Monomers and Polymers[a]

	$E_{on,m}$ (V)[b]	$E_{p,m}$ (V)	$E_{p,ox}$ (V)[c]	$E_{p,red}$ (V)[c]	$E_{1/2}$ (V)[c]	E_g (eV)
BProDOT-Me_2-$B(OC_{12}H_{25})_2$	0.44	0.55	0.25	−0.01	0.12	2.1
BProDOT-Hex_2-$B(OC_{12}H_{25})_2$	0.4	0.52	0.16	−0.04	0.06	2.1

[a] All potentials reported vs Fc/Fc^+. [b] $E_{on,m}$ = onset of monomer oxidation. [c] Scan rate = 100 mV s^{-1}.

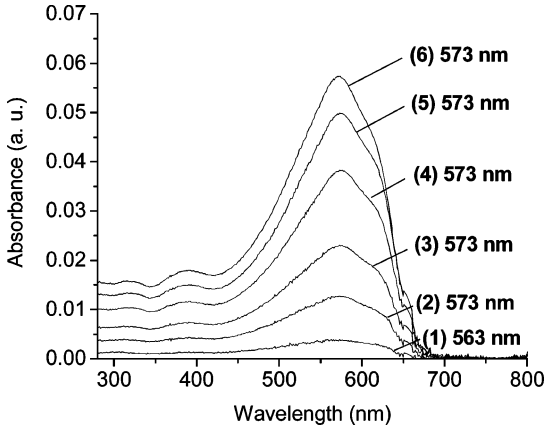

Figure 4. Absorption spectra for molecular weight fractions of PBProDOT-Hex_2-$B(OC_{12}H_{25})_2$. Molecular weights are reported in g mol^{-1} vs peak values for polystyrene: (1) 18 900, (2) 25 000, (3) 30 350, (4) 38 400, (5) 46 700, and (6) 61 500.

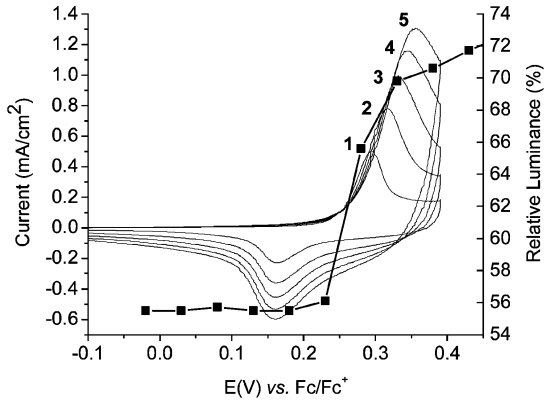

Figure 5. Cyclic voltammograms of PBProDOT-Hex_2-$B(OC_{12}H_{25})_2$ deposited on Pt button electrode, in 0.1 M TBAP/propylene carbonate electrolyte as a function of scan rate: (1) 100, (2) 150, (3) 200, and (4) 250 mV s^{-1}. Each spectrum is superimposed with % relative luminance vs applied potential (■) for PBProDOT-Hex_2-$B(OC_{12}H_{25})_2$.

monitoring polymer absorption as a function of molecular weight. For fractions with MW higher than polystyrene equivalents of 25 000 g mol^{-1}, the optimum optical conditions are attained, and the absorption maximum is at 573 nm. The narrow MW seen in the GP chromatogram indicates that the polymer does not contain low-MW oligomers (see Supporting Information). Interestingly, the absorption spectrum of the polymer in THF is red-shifted compared to the absorption spectrum in toluene (vide post). Therefore, THF is not as good a solvent as toluene for this polymer and induces twisting of the backbone to a more planar and rigid conformation. More details on the solvent effect will be given in the solvatochromism section.

Redox Properties of Chemically Synthesized PBProDOT-Hex_2-$B(OC_{12}H_{25})_2$. A film of PBProDOT-Hex_2-$B(OC_{12}H_{25})_2$ was deposited by drop-casting on a Pt button electrode from a 10 mg mL^{-1} chloroform solution, and cyclic voltammograms were recorded for different scan rates in 0.1 M TBAP/propylene carbonate electrolyte as illustrated in Figure 5 and compared to the electrochemically synthesized films. The polymer exhibits an $E_{1/2}$ of +0.23 V at 100 mV s^{-1}, which is a bit higher than the value obtained for the electropolymerized film, but not surprisingly different due to the different morphologies one would expect to form for the two film preparation methods. A linear relationship is found between the peak current and the scan rate, indicating that the polymer is electroactive and bound to the electrode.

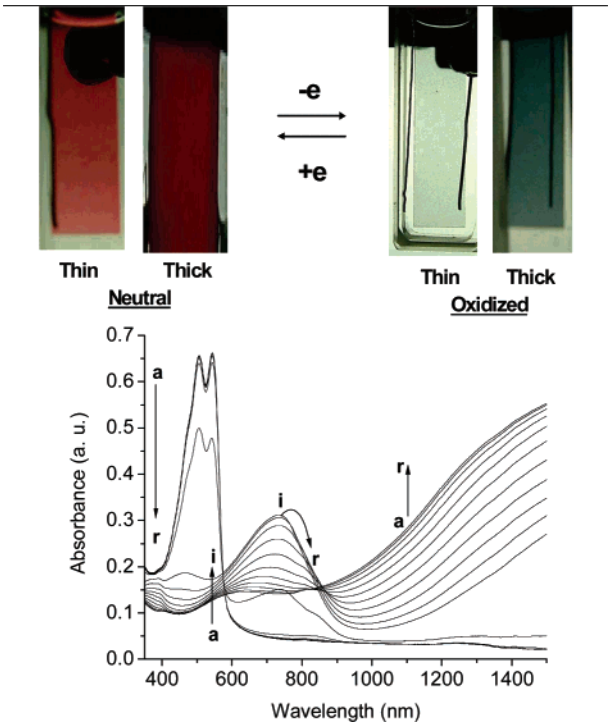

Figure 6. Spectroelectrochemical analysis of PBProDOT-Hex_2-$B(OC_{12}H_{25})_2$ spray cast on ITO-coated glass: UV−vis−NIR spectra taken (a) in the neutral state and at potentials of (b) −0.02 V, (c) +0.03 V, (d) +0.08 V, (e) +0.13 V, (f) +0.18 V, (g) +0.23 V, (h) +0.28 V, (i) +0.33 V, (j) +0.38 V, (k) +0.43 V, (l) +0.48 V, (m) +0.53 V, (n) +0.58 V, (o) +0.63 V, (p) +0.68 V, (q) +0.73 V, and (r) +0.78 V vs Fc/Fc^+ in 0.1 M TBAP/propylene carbonate. The film colors are displayed on top of the spectra for thin and thick films.

Spectroelectrochemistry. The chemically prepared PBProDOT-Hex_2-$B(OC_{12}H_{25})_2$ was studied by spectroelectrochemistry after film deposition by spray-casting onto indium tin oxide (ITO-coated) glass from a 10 mg mL^{-1} chloroform solution using an air brush (Testor Corps) at 12 psi. A highly homogeneous film was obtained and dried under vacuum. The spectra were recorded in 0.1 M TBAP in propylene carbonate in the neutral state, and stepping the potential from −0.02 to +0.78 V every 0.05 V, as shown in Figure 6.

The polymer exhibits an orange-red color in the neutral state with two absorption maxima at 544 and 507 nm (Figure 6a) which can be attributed to vibronic coupling. Upon oxidation, the $\pi-\pi^*$ transition of the neutral state disappears, and as soon as the potential reaches about +0.3 V, a polaron transition appears in the 600−800 nm region with a maximum absorption at 738 nm, changing the film color to light blue (Figure 6i). Upon further increase in potential, this transition progressively disappears, and bipolaron transitions are observed (1500 nm peaks) (Figure 6, i−r), and the polymer film becomes highly transmissive with a light gray color. This demonstrates the potential utility of this polymer in electrochromic applications.

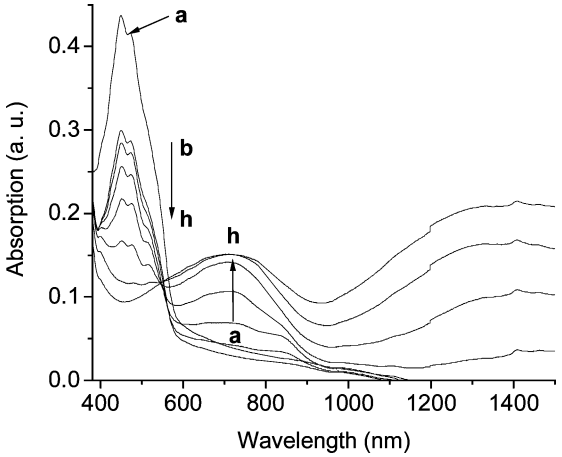

Figure 7. Spectroelectrochemical analysis of PBProDOT-Me_2-$B(OC_{12}H_{25})_2$ electropolymerized on ITO-coated glass: UV−vis-NIR spectra taken (a) in the neutral state and at potentials of (b) −0.28 V, (c) −0.08 V, (d) +0.02 V, (e) +0.12 V, (f) +0.22 V, (g) +0.32 V, and (h) +0.42 V vs Fc/Fc^+ in 0.1 M TBAP/propylene carbonate.

Polymer overoxidation and decomposition seemed to occur above +0.9 V. An optical band gap of 2.1 eV was determined from the onset of absorption of the neutral polymer.

For comparison, a thin film of PBProDOT-Me_2-$B(OC_{12}H_{25})_2$ was potentiostatically deposited onto an ITO-coated glass electrode at +0.5 V for 50 s using the same electrolyte and concentration as used for the electropolymerization on the Pt button. After washing with CH_2Cl_2/CH_3CN (3/5) solution, the orange polymer film was placed in a 0.1 M TBAP/propylene carbonate electrolyte solution, and various absorption spectra were recorded in the neutral state and at stepped potentials sequentially from −0.28 to +0.42 V oxidizing the polymer progressively (Figure 7). Overoxidation seemed to occur at higher potentials and the polymer film started to fall off the ITO electrode. As with PBProDOT-Hex_2-$B(OC_{12}H_{25})_2$, PBProDOT-Me_2-$B(OC_{12}H_{25})_2$ exhibits an optical band gap of 2.1 eV and a similar color change during redox switching, supporting our previous statement that the hexyl chains introduce little or no change in the optical properties. Surprisingly, the two PBProDOT-R_2-$B(OC_{12}H_{25})_2$ polymers exhibit the same band gaps as the recently studied poly(1,4-bis(2-thienyl)-2,5-diheptoxybenzene).[6] This result brings out the subtleties of the effect of side chains on the optical properties of π-conjugated polymers. In this instance, the thienylene-linked polymers may be packing in an even more regular manner in the solid state than the polymers studied here.

Colorimetry. A thin film of PBProDOT-Hex_2-$B(OC_{12}H_{25})_2$ was deposited on ITO by spray casting from a 10 mg mL^{-1} chloroform solution and was analyzed by in-situ colorimetric analysis.[20,21] The relative luminance (the brightness of the transmitted light as a percentage of the brightness of the light source) was measured as the neutral polymer was progressively oxidized, representative of the changes in light transmission with doping level. The spectrum is superimposed in Figure 5 onto the cyclic voltammetry results to compare the optical changes along with the material oxidation. Optical changes start occurring at +0.2 V vs Fc/Fc^+, which corresponds to the polymer oxidation. At this potential, there is a sharp increase in the luminance which goes from 55% to 70% in less than 0.1 V. Finally, upon further oxidation the luminance reaches saturation at +0.6 V.

The $L^*a^*b^*$ values of the colors were also determined to allow color matching. In the red-orange neutral state $L^* = 79$, $a^* = 40$, $b^* = 14$, and in the fully oxidized light gray state $L^* = 90$, $a^* = -1$, and $b^* = -3$ for a spray-cast film of about 0.2 μm in thickness. The available color states that PBProDOT-Hex_2-$B(OC_{12}H_{25})_2$ has to offer were also tracked using the *xy* chromaticity diagram shown in Figure 8.[20] As the potential is increased and the polymer is doped, the *x* coordinate decreases and the *y* coordinate decreases after an initial increase. The abrupt color change which occurs at +0.23 V and was observed on the luminance spectrum in Figure 6 can also be clearly seen on the *xy* chromaticity diagram by a large change in the *xy* coordinates at that potential. A few differences were observed for thicker films, such as a more pronounced blue color in the oxidized state (Figure 6), a lower luminance value (around 30%) characteristic of a more opaque film, and no difference in the luminance value between the neutral and the fully oxidized states.

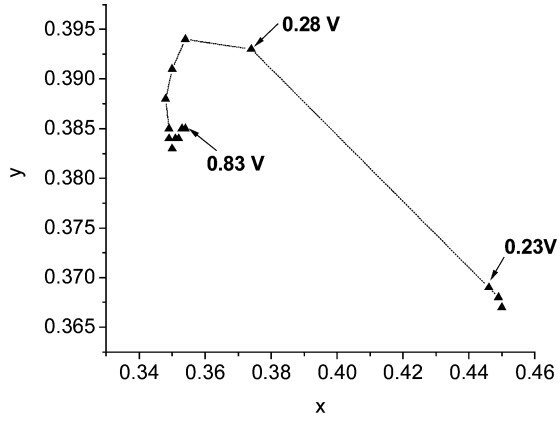

Figure 8. CIE 1931 *xy* chromaticity diagram. Triangles linked by a dashed line represent the color track for a thin film of PBProDOT-Hex_2-$B(OC_{12}H_{25})_2$ which goes from orange to light gray.

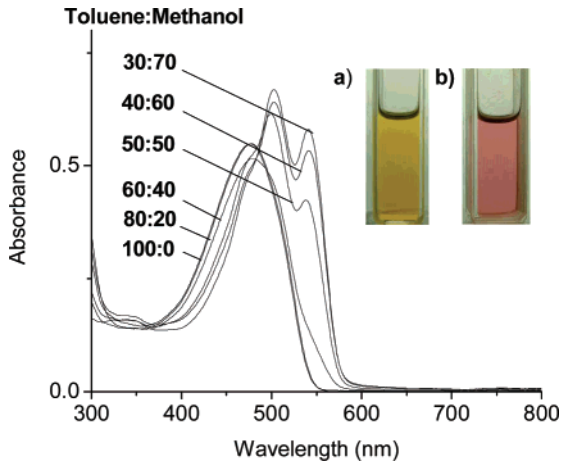

Figure 9. UV−vis absorption spectra of PBProDOT-Hex_2-$B(OC_{12}H_{25})_2$ in toluene/methanol mixtures. Pictures: solutions (a) in toluene and (b) in a mixture of toluene and methanol.

Solvatochromism. At room temperature, a 1.36×10^{-5} mol L^{-1} toluene solution of PBProDOT-Hex_2-$B(OC_{12}H_{25})_2$ is yellow and exhibits an absorption maximum at 478 nm, as illustrated in Figure 9. The resolution of the fine structure is not as well-defined as it is in the film absorption spectrum (Figure 6), and the solution absorption is blue-shifted compared to the film absorption where the maximum is observed at 544 nm. This is expected since solvated polymer chains are more disordered in solution and consequently have a lower conjugation length.

Upon addition of methanol, while maintaining a constant polymer concentration (1.36×10^{-5} mol L^{-1}), the solution becomes more red and shows a maximum absorption at 503

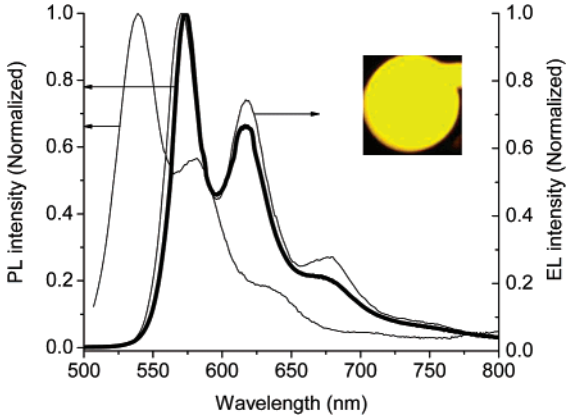

Figure 10. Photoluminescence emission spectrum of PBProDOT-Hex_2-$B(OC_{12}H_{25})_2$ in toluene solution and in thin film (bold line) superimposed with electroluminescence spectrum of an EL device with the following configuration: ITO/PEDOT-PSS/PBProDOT-Hex_2-$B(OC_{12}H_{25})_2$/Ca/Al. The inset picture represents the light emission of the EL device.

nm, with a vibronic sideband at 541 nm. In pure toluene, the polymer is highly solvated and poorly ordered. Upon addition of methanol, the polymer exhibits more extensive conjugation as can be deducted from the shift of the absorption maximum to longer wavelengths. According to the literature, the energy difference of 0.18 eV (1460 cm^{-1}) from the main peak to the vibronic peak is consistent with a C═C stretching mode, which would be expected to couple strongly to the electronic structure.[22] This is an additional evidence for the presence of more ordered molecules in the presence of poorly solvating solvents.

Light Emission. PBProDOT-Hex_2-$B(OC_{12}H_{25})_2$ exhibits yellow-orange fluorescence in toluene with an evaluated quantum efficiency of 54% (against Coumarin 6 standard; $\Phi = 0.78$).[23] The emission spectrum illustrated in Figure 10 exhibits two well-defined vibronic bands at 539 and 582 nm and one poorly resolved band at ~630 nm in toluene. For a spin-coated film, the emission spectrum has a similar shape although it is red-shifted due to a more organized conformation (Figure 10). The vibronic bands are seen at 571, 617, and 679 nm (photoluminescence quantum efficiency (PLQE) = 3.5 ± 2%).

Polymer light-emitting diodes (PLEDs) were prepared with the following architecture: ITO/PEDOT-PSS (40 nm)/PBProDOT-Hex_2-$B(OC_{12}H_{25})_2$ (50 nm)/Ca (5 nm)/Al (200 nm). As shown in Figure 10, the device exhibits a broad emission dominated by a peak at $\lambda_{max} = 570$ nm. The electroluminescence (EL) spectrum is similar to the photoluminescence (PL) spectrum of the solid film (Figure 10), indicating that the electroluminescence results from a singlet π,π^* exciton with the same structure as that produced by photoexcitation. The absence of red-shifting on the EL spectrum relative to the PL spectrum suggests that the electroluminescence is dominated by the nonaggregated polymer chains, with the interchain aggregates contributing to little or no emission.

The application of PBProDOT-Hex_2-$B(OC_{12}H_{25})_2$ in LEDs was evaluated. Considering the device characteristics illustrated in Figure 11, the PBProDOT-Hex_2-$B(OC_{12}H_{25})_2$ device turns on at 6 V. The EL intensity increases with voltage, peaking at 13 V, and decreasing at higher voltages, possibly due to device breakdown. At 13 V, the device emits the highest luminance at ~240 cd m^{-2} and current density of 1100 mA cm^{-2}. Figure 11 shows the external electron-to-photon quantum efficiency of the PBProDOT-Hex_2-$B(OC_{12}H_{25})_2$ EL device as a function of applied voltage. The efficiency increases after turn on, peaking at 8 V at ~0.03%, after which it steadily decreases as the applied voltage and current density increase.

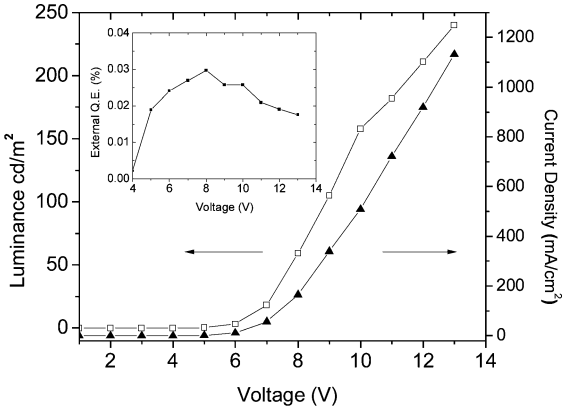

Figure 11. Luminance spectrum of PBProDOT-Hex_2-$B(OC_{12}H_{25})_2$ (□) and current density (▲). Left top inset: external quantum efficiency of PBProDOT-Hx_2-$B(OC_{12}H_{25})_2$ device.

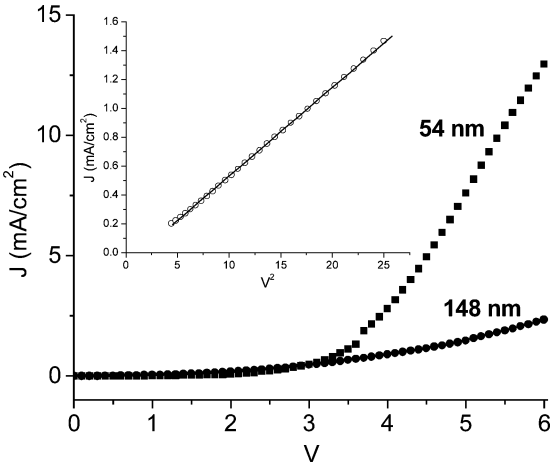

Figure 12. Current−voltage ($J-V$) characteristics of devices comprising PBProDOT-Hex_2-$B(OC_{12}H_{25})_2$ as the active hole transporting layer. Inset shows the $J-V^2$ plot for the 148 nm thick polymer, between 2 and 5 V, along with its linear fit.

Hole Transport Properties. The hole transport properties of the PBProDOT-Hex_2-$B(OC_{12}H_{25})_2$ thin films have been investigated by fabricating hole-dominated devices and fitting the current−voltage curves to the space charge limited current (SCLC) model.[24,25] Devices of the following structure have been prepared: ITO/PEDOT-PSS/polymer/Au. Because of the high energy barrier between Au (~4.8 eV) and the LUMO level of the polymer (3.2 eV, assuming SCE at 4.7 eV below the vacuum level),[26] the current measured is mainly hole dominated.

At voltages above 2 V up to 6 V, the hole-dominated devices showed SCLC and follow $J = {}^9/_8\epsilon_r\epsilon\mu_h(V^2/L^3)$, where J is the current density, V is the applied voltage, μ_h is the hole mobility, L is the thickness of the polymer layer, and ϵ_r and ϵ are the permittivity of the polymer and air, respectively.[24,25] The voltage has been corrected by subtracting the voltage drop due to the contact resistance (~60 Ω), which was obtained from the $J-V$ curve of a device without the polymer layer.

Figure 12 shows the $J-V$ characteristics of hole-dominated devices in the forward-bias (PEDOT-PSS as the hole injector) with two different polymer thickness values of 54 and 148 nm. Hole mobilities were derived from the linear slope of J vs V^2 curves as shown in the inset for the 148 nm thick polymer device. The hole mobility values were calculated to be (2.8 ± 0.02) × 10^{-7} and (6.8 ± 0.23) × 10^{-6} cm^2 V^{-1} s^{-1} for the 54 nm and the 148 nm polymer device, respectively, the higher

value being comparable to the hole mobility measured for low molecular weight regioregular poly(3-hexylthiophene) diodes.[24] Reverse-biased devices showed similar $J-V$ curves (see Supporting Information), except that the turn-on voltages were slightly higher possibly due to the lower work function of the Au layer compared to the PEDOT-PSS.

Conclusion

The family of thienylene−phenylene-based copolymers has been broadened with the introduction of ProDOT heterocycles, giving rise to new possibilities in the field of organic electronics. The crystalline packing with a small interchain distance of the three-ring BProDOT-Me_2-$B(OC_{12}H_{25})_2$ system suggests the potential of this type of molecule for electronic applications requiring high charge carrier mobility, and one can imagine the development of oligomers of this type for applications such as field effect transistors. The hole mobility of PBProDOT-Hex_2-$B(OC_{12}H_{25})_2$ has been investigated in the SCLC regime, showing that the polymer exhibits potentially useful hole transport properties and is currently under investigation by our group for organic photovoltaic devices.

The PBProDOT-R_2-$B(OC_{12}H_{25})_2$ polymers exhibit band gaps of 2.1 eV, quite close to their thiophene counterparts likely due to a less regular packing in the solid state. This in turn compensates the electron-donating effect of the oxygen substituents appended to the thiophene ring and gives rise to films having a similar orange color in the neutral state.[27] Conversely, as the polymer is progressively oxidized, a different behavior is observed for PBProDOT-Hex_2-$B(OC_{12}H_{25})_2$ and a highly transmissive state is reached while the thiophene analogues retain a deeper blue color.[6,27] A chemical synthesis was developed for this polymer, giving rise to a highly soluble material that can be processed by spray-casting or spin-coating techniques. These interesting solubility and color switching properties open the door to electrochromic applications using large or flexible surfaces such as electrochromic displays or smart windows.

Experimental Section

Instrumentation. ^{1}H NMR and ^{13}C NMR spectra were recorded on Varian-VXR 300 MHz, Gemini 300 MHz, and Mercury 300 MHz using $CDCl_3$ and were referenced to the solvent residual peak (^{1}H: 7.27 ppm; ^{13}C: 77.23). Elemental analyses were performed by Robertson Microanalytical Laboratories, Inc., or the University of Florida, Department of Chemistry spectroscopic services. High-resolution mass spectrometry was performed by the spectroscopic services at the Department of Chemistry of the University of Florida with a Finnigan MAT 96Q mass spectrometer. GPC was performed on two 300 × 7.5 mm Polymer Laboratories PLGel 5 μM mixed-C columns with a Waters Associates liquid chromatography 2996 photodiode array detector. All molecular weights are relative to polystyrene standards (Polymer Laboratories, Amherst, MA). The polymer solutions were prepared in THF, and a constant flow rate of 1 mL min^{-1} was used. MALDI-TOF mass spectrometry was performed with a Bruker ProFLEX III instrument at Louisiana State University. Methylene chloride was used as solvent and terthiophene as matrix. Electrochemistry was performed using a three-electrode cell with a platinum wire or a Pt flag as the counter electrode, an Ag wire pseudo-reference electrode calibrated using a 5 mM solution of Fc/Fc^+ in 0.1 M electrolyte solution, and a platinum button or ITO-coated glass slide (7 × 50 × 0.7 mm, 20 Ω cm^{-1}) as the working electrode. The ITO electrodes were purchased from Delta Technologies, Ltd. All potentials were reported vs Fc/Fc^+. Characterization of the polymer films was performed in 0.1 M electrolyte solution. An EG&G Princeton Applied Research model 273 potentiostat was used under the control Corrware II software from Scribner and Associates. All absorption spectra from solvatochromism and optoelectrochemical studies were performed using a Varian Cary 500 Scan UV−vis−near-IR spectrophotometer. Colorimetry measurements were obtained using a Minolta CS-100 Chroma Meter. The sample was illuminated from behind with a D50 (5000K) light source in a light booth designed to exclude external light. Photoluminescence spectra were registered on a Jobin Yvon Fluorolog-3 spectrofluorimeter in right-angle mode for solutions and using front-face geometry for films. Solution quantum efficiency measurements were carried out relative to Coumarin 6 in ethanol where $\Phi = 0.78$, with the optical density of the solution kept below $A = 0.1$, using a Spex F-112 photon counting fluorimeter. The polymer film for PLQE measurement was prepared by spin-coating a solution of PBProDOT-Hex_2-$B(OC_{12}H_{25})_2$ (10 mg mL^{-1} in 1,2-dichloroethane) onto a glass substrate to make a ∼500 Å thick film. The resulting film was dried under vacuum (10^{-6} Torr) for 12 h at room temperature. The PLQE measurements were made following procedures described in the literature[28] using an integrating sphere (Oriel) connected to an ISA-SPEX Triax 180 spectrometer fitted with a liquid nitrogen cooled CCD detector and exciting with a tungsten lamp. Electroluminescent devices were prepared by first masking and then etching ITO glass (Delta Technologies, $R_s = 8-12$ Ω). After etching, the ITO glass was sequentially cleaned by sonication in sodium dodecyl sulfate, Milli-Q water, acetone, and isopropyl alcohol and then plasma (oxygen) treated for 15 min. A 400 Å thick hole transport layer of PEDOT-PSS (Bayer Baytron P VP Al 4083) was spin-coated onto the ITO surface and dried in a vacuum at 150 °C for 4 h. Solutions of the PBProDOT-Hex_2-$B(OC_{12}H_{25})_2$ polymer (10 mg mL^{-1} in 1,2-dichloroethane) were spin-coated onto the substrate (300 μL for each substrate) to make ∼500 Å thick films. The resulting films were dried under vacuum (10^{-6} Torr) for 12 h at room temperature, and then Ca (50 Å) and Al (2000 Å) layers were deposited by thermal evaporation at 4×10^{-7} Torr without breaking the vacuum between metal depositions. The resulting devices were encapsulated with epoxy (Loctite quick-set) to minimize exposure to oxygen and moisture. All device measurements were prepared at room temperature. For the EL device characterization, the power was supplied using a Keithley 228 voltage−current source. EL spectra were corrected on an ISA-SPEX Triax 180 spectrometer fitted with a liquid N_2-cooled CCD detector (Hamamatsu back-illuminated CCD, 1024 × 64 pixel, 400−1100 nm). Measurements were made normal to the surface of the devices, and in the computation of the EL quantum efficiencies it was assumed that the spatial distribution of the emission was Lambertian.[28] External device quantum efficiencies were calculated as described in the literature.[29] Hole-dominated devices were fabricated the same way as LEDs but using Au (80 nm) as the top contact to prevent electron injection. Current−voltage characteristics of the devices were measured at room temperature using a Keithley 228 source meter, and the mobility values were determined from the $J-V^2$ curve above 2.5 V. A device without the semiconductor polymer layer (ITO/PEDOT-PSS/Au) was fabricated and tested to determine the series resistance (∼60 Ω).

X-ray Crystallography: Data Collection, Structure Solution, and Refinement. Data were collected at 173 K on a Siemens SMART PLATFORM equipped with a CCD area detector and a graphite monochromator utilizing Mo Kα radiation ($\lambda = 0.71073$ Å). Cell parameters were refined using up to 8192 reflections. A full sphere of data (1850 frames) was collected using the ω-scan method (0.3° frame width). The first 50 frames were remeasured at the end of data collection to monitor instrument and crystal stability (maximum correction on I was < 1%). Absorption corrections by integration were applied based on measured indexed crystal faces. The structure was solved by the Direct Methods in SHELXTL6 (2000, Bruker-AXS, Madison, WI) and refined using full-matrix least squares. The non-H atoms were treated anisotropically, whereas the hydrogen atoms were calculated in ideal positions and were riding on their respective carbon atoms. The molecules lie on inversion centers; thus, half the molecule is found in the asymmetric unit. A total of 253 parameters were refined in the final cycle of refinement using 2881 reflections with $I > 2\sigma(I)$

to yield R_1 and wR_2 of 4.69% and 11.58%, respectively. Refinement was done using F^2.

Materials. All chemicals were purchased from Fisher Scientific and used as received unless stated otherwise. Tetrahydrofuran (THF), *N*-methyl-2-pyrrolidinone (NMP), CH_2Cl_2, and CH_3CN were dried and distilled prior to use. Tetrabutylammonium perchlorate (TBAP) was recrystallized from 2-propanol. Tris(dibenzylideneacetone)dipalladium ($Pd_2(dba)_3$) was purchased from Strem and used as received. Tri-*tert*-butylphosphine [P(*t*-Bu)$_3$] and zinc chloride were purchased from Aldrich Chemicals, and P(*t*-Bu)$_3$ was manipulated in a drybox. 1,4-Dibromo-2,5-didodecyloxybenzene,[5] 3,3-dihexyl-3,4-dihydro-2*H*-thieno[3,4-*b*][1,4]dioxepine (ProDOT-Hex$_2$),[30] and 3,3-dimethyl-3,4-dihydro-2*H*-thieno[3,4-*b*][1,4]dioxepine (ProDOT-Me$_2$)[31] were synthesized using known procedures.

1,4-Bis[3,3-dihexyl-3,4-dihydro-2*H*-thieno[3,4-*b*][1,4]dioxepin-6-yl]-2,5-didodecyloxybenzene (1). 3,3-Dihexyl-3,4-dihydro-2*H*-thieno[3,4-*b*][1,4]dioxepine (ProDOT-Hex$_2$) (6.34 g, 2.0×10^{-2} mol) was dissolved in anhydrous THF (100 mL) in a 500 mL three-neck round-bottom flask equipped with a condenser under nitrogen. The solution was cooled to −78 °C, *n*-BuLi (2.1×10^{-2} mol) was added dropwise via syringe, and the solution was stirred for 1 h at −78 °C. Zinc chloride in THF (2.3×10^{-2} mol) was added dropwise via syringe, and the solution was warmed to room temperature followed by addition via cannula of anhydrous NMP (100 mL). 1,4-Dibromo-2,5-didodecyloxybenzene (4.83 g, 8.0×10^{-3} mol), $Pd_2(dba)_3$ (0.29 g, 3.2×10^{-4} mol), and P(*t*-Bu)$_3$ (1.29×10^{-1} g, 6.4×10^{-4} mol) were dissolved in anhydrous THF (100 mL) and anhydrous NMP (100 mL) in a Schlenk flask. This purple solution was transferred via cannula to the solution containing the zinc chloride derivative of ProDOT-Hex$_2$, and the mixture was heated at 100 °C for 12 h. The light brown solution was cooled to room temperature and poured into deionized water (300 mL). The mixture was extracted with ethyl ether; the ether layer was washed with brine and dried over magnesium sulfate. After filtration through a Büchner funnel, the solvent was evaporated and a yellow oil collected. This oil was purified by column chromatography (1:3, benzene, hexanes) and dried under vacuum to give 3.82 g (44%) of a yellow solid; mp 45−46 °C. ^{1}H NMR ($CDCl_3$): δ 7.50 (s, 1H), 6.45 (s, 1H), 3.99 (t, 2H), 3.90 (s, 2H), 3.91 (s, 2H), 1.82 (p, 2H), 1.39 (m, 4H), 1.27 (m, 34H), 0.88 (m, 9H). ^{13}C NMR ($CDCl_3$): δ 149.6, 149.3, 146.5, 121.6, 117.8, 114.7, 104.1, 69.9, 43.9, 32.3, 32.1, 32.0, 30.4, 29.9, 29.9, 29.8, 29.7, 29.6, 26.4, 23.1, 22.9, 22.8, 14.3, 14.2. HRMS: calcd for $C_{68}H_{114}O_6S_2$: 1090.8057. Found: 1090.8070. Anal. Calcd for $C_{68}H_{114}O_6S_2$: C, 74.81; H, 10.52. Found: C, 74.62, H, 10.64.

1,4-Bis[3,3-dimethyl-3,4-dihydro-2*H*-thieno[3,4-*b*][1,4]dioxepin-6-yl]-2,5-didodecyloxybenzene (2). 3,3-Dimethyl-3,4-dihydro-2*H*-thieno[3,4-*b*][1,4]dioxepine (ProDOT-Me$_2$) (5.00 g, 2.7×10^{-2} mol) was dissolved in anhydrous THF (150 mL) in a 1 L three-neck round-bottom flask equipped with a condenser under nitrogen. The solution was cooled to −78 °C, *n*-BuLi (2.9×10^{-2} mol) was added dropwise via syringe, and the solution was stirred for 1 h at −78 °C. Zinc chloride in THF (3.1×10^{-2} mol) was added dropwise via syringe, and the solution was warmed to room temperature followed by addition via cannula of anhydrous NMP (200 mL). Then, 1,4-dibromo-2,5-didodecyloxybenzene (5.48 g, 9.0×10^{-3} mol), $Pd_2(dba)_3$ (0.33 g, 3.6×10^{-4} mol), and P(*t*-Bu)$_3$ (1.46×10^{-1} g, 7.2×10^{-4} mol) were dissolved in anhydrous THF (100 mL) and anhydrous NMP (50 mL) in a Schlenk flask. This purple solution was transferred via cannula to the solution containing the zinc chloride derivative of ProDOT-Me$_2$, and the mixture was heated at 100 °C for 12 h. The light brown solution was cooled to room temperature and poured into deionized water (500 mL). The mixture was extracted with ethyl ether; the ether layer was washed with brine and dried over magnesium sulfate. After filtration through a Büchner funnel, the solvent was evaporated and a light brown solid collected. This solid was purified by column chromatography (1:1, benzene, hexanes) followed by recrystallization (1:5, ethyl acetate, hexanes) to give 3.02 g (42%) of yellow crystals; mp 80−82 °C. ^{1}H NMR ($CDCl_3$): δ 7.49 (s, 1H), 6.53 (s, 1H), 4.01 (t, 2H), 3.81 (s, 2H), 3.79 (s, 2H), 1.84 (p, 2H), 1.47 (m, 2H), 1.27 (m, 16H), 1.07 (s, 6H), 0.88 (t, 3H). ^{13}C NMR ($CDCl_3$): δ 149.9, 149.5, 146.8, 121.8, 118.7, 114.9, 104.9, 80.3, 80.1, 70.0, 39.1, 32.1, 29.9, 29.8, 29.7, 29.6, 29.5, 26.4, 22.9, 22.0, 14.3. HRMS: calcd for $C_{48}H_{74}O_6S_2$: 810.4927. Found: 810.4928. Anal. Calcd for $C_{48}H_{74}O_6S_2$: C, 71.07; H, 9.19. Found: C, 71.16, H, 9.38.

Poly[1,4-Bis[3,3-dihexyl-3,4-dihydro-2*H*-thieno[3,4-*b*][1,4]-dioxepin-6-yl]-2,5-didodecyloxybenzene] (3). Compound **1** (0.80 g, 7.3×10^{-4} mol) was dissolved in chloroform (15 mL) under nitrogen. A slurry of iron chloride (0.36 g, 2.2×10^{-3} mol) in chloroform (15 mL) was added dropwise to the monomer solution over a 2 h period. With addition of oxidant, the yellow solution turned dark purple. The mixture was stirred overnight at room temperature and then precipitated into methanol (500 mL). The precipitate was filtered through a Soxhlet thimble and redissolved in chloroform (250 mL) where it was stirred for 6 h with excess hydrazine monohydrate (10 mL). The solution was concentrated by evaporation, and the polymer solution was poured into methanol (400 mL) where a red precipitate formed. The precipitate was filtered through a Soxhlet thimble, purified via Soxhlet extraction for 18 h with methanol, and extracted for 8 h with chloroform. The solvent was evaporated from the chloroform fraction and a red solid collected (0.74 g, 92%). ^{1}H NMR ($CDCl_3$, ppm): δ = 7.61 (b, 1H), 3.96−4.06 (b, 6H), 1.92 (b, 2H), 1−1.50 (bm, 38H), 0.88 (bm, 9H). GPC analysis: M_n = 14 600, M_w = 22 990, PDI = 1.57. Anal. Calcd for $C_{68}H_{112}O_6S_2$: C, 74.94; H, 10.35; S, 5.88. Found: C, 70.90; H, 10.59; S, 4.73; Cl, 0.13; Fe, 0.22.

Acknowledgment. This work was supported by grants from AFOSR (FA955-06-1-0192) and EIC (NASA-NNC05CB23C). K.A.A. wishes to acknowledge the National Science Foundation and the University of Florida for funding of the purchase of the X-ray equipment. T.D.M. wishes to thank the NSF for funding (CHE-0074884).

Supporting Information Available: Listings of crystal data and structure refinement parameters, atomic coordinates, bond lengths and angles, anisotropic displacement parameters, hydrogen coordinates, and isotropic displacement parameters for BProDOT-Me$_2$-B(OC$_{12}$H$_{25}$)$_2$; ^{1}H NMR of BProDOT-Hex$_2$-B(OC$_{12}$H$_{25}$)$_2$ and PBProDOT-Hex$_2$-B(OC$_{12}$H$_{25}$)$_2$; GPC spectra of PBProDOT-Hex$_2$-B(OC$_{12}$H$_{25}$)$_2$; and reverse bias *J*−*V* curves of hole-dominated devices. This material is available free of charge via the Internet at http://pubs.acs.org.

References and Notes

(1) Wang, F.; Wilson, M. S.; Rauh, R. D.; Schottland, P.; Thompson, B. C.; Reynolds, J. R. *Macromolecules* **2000**, *33*, 2083−2091.
(2) Tada, K.; Onoda, M.; Yoshino, K. *J. Phys. D: Appl. Phys.* **1997**, *30*, 2063−2068.
(3) Pei, J.; Yu, W.-L.; Ni, J.; Lai, Y.-H.; Huang, W.; Heeger, A. J. *Macromolecules* **2001**, *34*, 7241−7248.
(4) Irvin, J. A.; Reynolds, J. R. *Polymer* **1998**, *39*, 2339−2347.
(5) Ruiz, J. P.; Dharia, J. R.; Reynolds, J. R.; Buckley, L. J. *Macromolecules* **1992**, *25*, 849−860.
(6) Child, A. D.; Sankaran, B.; Larmat, F.; Reynolds, J. R. *Macromolecules* **1995**, *28*, 6571−6578.
(7) Sotzing, G. A.; Reynolds, J. R.; Steel, P. J. *Chem. Mater.* **1996**, *8*, 882−889.
(8) Irvin, J. A.; Piroux, F.; Morvant, M. C.; Robertshaw, V. L.; Angerhofer, A.; Reynolds, J. R. *Synth. Met.* **1999**, *102*, 965−966.
(9) Bao, Z.; Chan, W.; Yu, L. *Chem. Mater.* **1993**, *5*, 2−3.
(10) Pelter, A.; Jenkins, I.; Jones, D. E. *Tetrahedron* **1997**, *53*, 10357−10400.
(11) Bouachrine, M.; Bouzakraoui, S.; Hamidi, M.; Ayachi, S.; Alimi, K.; Lère-Porte, J.-P.; Moreau, J. *Synth. Met.* **2004**, *145*, 237−243.
(12) Mushursh, M.; Facchetti, A.; Lefenfeld, M.; Katz, H. E.; Marks, T. J. *J. Am. Chem. Soc.* **2003**, *125*, 9414−9423.
(13) Xu, M.-H.; Zhang, H.-C.; Pu, L. *Macromolecules* **2003**, *36*, 2689−2694.
(14) Pavlishchuk, V. V.; Addison, A. W. *Inorg. Chim. Acta* **2000**, *298*, 97−102.
(15) Reeves, B. D.; Grenier, C. R. G.; Argun, A. A.; Cirpan, A.; McCarley, T. D.; Reynolds, J. R. *Macromolecules* **2004**, *37*, 7559−7569.

(16) Kumar, A.; Welsh, D. M.; Morvant, M. C.; Piroux, F.; Abboud, K. A.; Reynolds, J. R. *Chem. Mater.* **1998**, *10*, 896−902.
(17) *Handbook of Conducting Polymers*; Skotheim, T. A., Ed.; Marcel Dekker: New York, 1986; Vol. 1, Chapter 9.
(18) Sankaran, B.; Reynolds, J. R. *Macromolecules* **1997**, *30*, 2582−2588.
(19) Dai, C.; Fu, G. C. *J. Am. Chem. Soc.* **2001**, *123*, 2719−2724.
(20) Thompson, B. C.; Schottland, P.; Sonmez, G.; Reynolds, J. R. *Synth. Met.* **2001**, *119*, 333−334.
(21) Thompson, B. C.; Schottland, P.; Zong, K.; Reynolds, J. R. *Chem. Mater.* **2000**, *12*, 1563−1571.
(22) Leclerc, M.; Dufresne, G.; Blondin, P.; Bouchard, J.; Belletête, M.; Durocher, G. *Synth. Met.* **2001**, *119*, 45−48.
(23) Reynolds, G. A.; Drexhage, K. H. *Opt. Commun.* **1975**, *13*, 222−225.
(24) Goh, C.; Kline, R. J.; McGehee, M. D.; Kadnikova, E. N.; Frechet, J. M. J. *Appl. Phys. Lett.* **2005**, *86*, 122110−122113.
(25) Benvenho, A. R. V.; Hummelgen, I. A. *Mater. Res.* **2001**, *4*, 133−136.
(26) Bard, A. J.; Faulkner, L. R. *Electrochemical Methods: Fundamentals and Applications*, 2nd ed.; Wiley: New York, 2001; p 54.
(27) Tada, K.; Onoda, M.; Yoshino, K. *J. Phys. D: Appl. Phys.* **1997**, *30*, 2063−2068.
(28) Greenham, N. C.; Samuel, I. D. W.; Hayes, G. R.; Phillips, R. T.; Kessener, Y. A. R. R.; Moratti, S. C.; Holmes, A. B.; Friend, R. H. *Chem. Phys. Lett.* **1995**, *241*, 89−96.
(29) Forrest, S. R.; Bradley, D. D. C.; Thompson, M. E. *Adv. Mater.* **2003**, *15*, 1043−1048.
(30) Mishra, S. P.; Krishnamoorthy, K.; Sahoo, R.; Kumar, A. *J. Polym. Sci., Part A: Polym. Chem.* **2005**, *43*, 419−428.
(31) Welsh, D. M.; Kumar, A.; Meijer, E. W.; Reynolds, J. R. *Adv. Mater.* **1999**, *11*, 1379−1382.

MA060466N